Available online at www.most.gov.bd

Volume 03, Issue (1), Page : 23-40, 2021

Ministry of Science and Technology
Government of The People's of Bangladesh
Bangladesh Secretariat, Dhaka.

Chemical Synthesis of Cytosine β-D-Riboside Esters for Pathogenicity, Anticancer and Computational Studies

S. M. A. Kawsar* and J. Ferdous

Laboratory of Carbohydrate and Nucleoside Chemistry (LCNC), Department of Chemistry, Faculty of Science, University of Chittagong, Bangladesh

Abstract

The growing importance of nucleoside derivatives as unique potential antimicrobial and therapeutic agents has drawn attention to the synthesis of thymidine derivatives. In the present study, cytidine (i.e., cytosine β-D-riboside) was treated with various acyl halides to produce 5′-*O*-acyl cytidine derivatives by direct acylation method with an excellent yield. To obtain newer derivatives for antimicrobial assessment studies, the 5′-*O*-cytidine derivatives were further modified into three series of 2′,3′-di-*O*-acyl cytidine derivatives (schemes 1 and 2) containing a wide variety of functionalities in a single molecular framework. The chemical structures of the newly synthesized derivatives were elucidated by analyzing their physicochemical, elemental, and spectroscopic data. The antimicrobial tests demonstrated that most of the derivatives exhibited significant antibacterial and antifungal activities *in vitro*. The derivatives **7**, **10**, and **11** were the most potent derivatives against *Pseudomonas aeruginosa*, *Salmonella abony*, and *Staphylococcus* strains, with the minimum inhibitory concentration ranging from 0.16 ± 0.01 to 1.25 ± 0.03 mg/mL and minimum bactericidal concentration ranging from 0.32 ± 0.01 to 2.5 ± 0.06 mg/mL. The strongest inhibitory activity was observed against Gram-negative bacteria. Some of the derivatives had a strong antifungal activity. The structure–activity relationship (SAR) and X-ray powder diffraction of these acylated products were also studied. In addition, derivative **6** exhibited good anticancer activity against EAC cells. Quantum chemical studies were performed employing density functional theory with B3LYP/3-21G level. To support this observation, molecular docking studies have been performed against HIV-1 reverse transcriptase (RT) (PDB: 3V4I). Most of the molecules studied out here could bind near the crucial catalytic binding site, Tyr181, Ile94, Ile382, Lys374, Val381, Val90, and Tyr34 of the HIV-1 reverse transcriptase (RT), and the molecules were surrounded by other active site residues like Gln332, Trp406, Asn265, Gly93, His96, Pro95, and Thr165. The absorption, distribution, metabolism, excretion, and toxicity properties predicted the improved pharmacokinetic properties of all derivatives.

Received: 17 January 2021
Revised: 16 May 2022
Accepted: 10 July 2022

DOI: https://doi.org/10.3329/JSciTR.v3i1.62804

Keywords: Synthesis; Cytosine β-D-Riboside; Spectroscopy; Anticancer; Computational

*Corresponding author e-mail: akawsarabe@yahoo.com

Introduction

Nucleosides and their derivatives are an important class of clinically useful medicinal agents that possess antiviral and anticancer activities (Katherine *et al.,* 2018). Nucleosides belong to a class of organic compounds that possess a nitrogen-containing heterocyclic nucleobase and a C-5 sugar as ribose or deoxyribose in their structure. The nucleobase is bound to the C-5 sugar (anomeric carbon) via a β-N-glycoside linkage (King 2006). Phosphorylation on the primary hydroxyl group of the sugar moiety results in the formation of nucleotides, which are the building blocks of DNA and RNA. Nucleosides and nucleotide derivatives are necessary for life as they are integral in a variety of cell metabolism and regulation processes. General nucleotide chemistry and investigations using both purine and pyrimidine nucleosides have contributed substantially to the discovery and elucidation of countless biological processes at the molecular level (Kukhanova 2012).

The nucleoside, cytidine (cytosine β-D-riboside, 1) (Fig. 1) is an essential component in RNA synthesis and plays an important role in the synthesis of glycogen. In addition, it contributes to the synthesis of bio-membranes via the formation of pyrimidine–lipid conjugates. Upon digestion of foods containing RNA, uridine is released from the RNA molecule and is absorbed intact in the gut. Cytidine acts as an antidepressant, alleviates asthmatic airway inflammation, and is the key to hepatocyte proliferation (Ichikawa and Kato 2001). Uridine is often administered as part of a cancer treatment regime to minimize the adverse effects of chemotherapy drugs like 5-fluorouracil (Groeningen *et al.,* 1986). Furthermore, a combination of uridine and benzylacyclouridine was shown to reduce neurotoxicity and bone marrow toxicity related to the drug zidovudine in the treatment of HIV (Morris, 1994). Despite these advances, the availability of novel, effective nucleoside derivatives for pharmaceutical purposes is still lacking, and research on this field remains of utmost importance (Jordheim *et al.,* 2013). To this end, a number of fruitful and efficient methods for selective acylation have been reported, in which a variety of acylating agents and reaction conditions were utilized to attain the desired derivatives in good yields (Tsuda and Haque *et al.,* 1983). As the 5′-OH (primary) is more reactive than 2′,3′-OH (secondary), selective acylation takes place according to the reactivity of hydroxyl (-OH) groups. Various methods for the acylation of carbohydrates and nucleosides have, so far, been developed and successfully employed (Kabir *et al.,* 2005; Ishji *et al.,* 1980).

The cytidine derivative KP-1461 is an anti-HIV agent that acts as a viral mutagen (Harris *et al.,* 2005). Alteration of hydroxyl (-OH) group at 3′ and 5′ position increases the antimicrobial activity of pyrimidine nucleoside and brings about some potent antimicrobial agents (Chowdhury *et al.,* 2019). As a result of screening synthetic derivatives for potential antimicrobial activity, a study reported that azidothymidine (AZT) has potent bactericidal in vitro activity against various members of the family Enterobacteriaceae. Azidothymidine (AZT) is also one of the most popular nucleoside derivatives (antiviral drug) in which 3′ hydroxyl (-OH) of thymidine is replaced by an azide group and used worldwide for the treatment of HIV infection (Krayevsky *et al.,* 1993). Various cytidine derivatives have been modified in the base/ribose and exhibited antiviral or antitumor activities. Furthermore, the alteration of the hydroxyl (-OH) group of nucleoside derivatives, uridine and cytidine also has potential antimicrobial activity (Bulbul *et al.,* 2021; Tanima *et al.,* 2019). Recently, some quantum chemical studies reported modified thymidine derivatives are also consisting of potent thermodynamic stability and pharmacological properties (Kawsar *et al.,* 2020).

In vitro antimicrobial properties of nucleosides that have been subjected for the selective acylation (Devi *et al.,* 2019; Jesmin *et al.,* 2017) and revealed that N, S, and X-containing substitution derivatives showed markedly better antimicrobial and biological activity than their parent compound (Kawsar *et al.,* 2014; Kabir *et al.,* 2004). Encouraged by the literature reports and our findings (Kawsar *et al.,* 2018; Arifuzzaman *et al.,* 2018), we focused on synthesizing a series of cytidine derivatives (schemes 1 and 2) that deliberately incorporated a wide variety of biologically active components into the ribose moiety. This was done in the hope of finding new antibacterial and antifungal potential agents. In this view, the potent antiviral efficacy of several cytidine derivatives 2–15 with various aliphatic and aromatic chains investigated by molecular docking against HIV-1 reverse transcriptase (RT) (PDB: 3V4I) along with B3LYP/3-21G level quantum chemical studies. The in vitro antimicrobial minimum inhibitory concentrations (MIC), minimum bactericidal concentrations (MBC), anticancer, SAR study, and computational studies of these newly synthesized cytidine derivatives are reported herein for the first time along with the search of anti-HIV drug candidates.

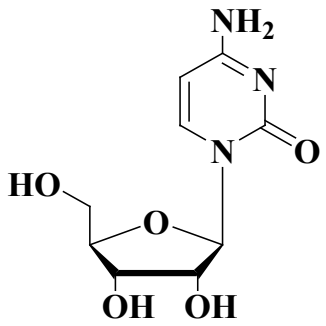

Fig. 1. Chemical structure of the cytidine

Materials and methods

Melting points (m.p.) were determined using an electrothermal melting point apparatus and were uncorrected. Evaporation was performed using a Büchi rotary evaporator under diminished pressure. Analytical grade solvents were employed and purified using standard procedures. Infrared (IR) spectral analyses were conducted using a Fourier transform IR (FTIR) spectrophotometer (IR Prestige-21, Shimadzu, Japan) within 200–4000 cm^{-1} at the Department of Chemistry, University of Chittagong, Bangladesh. A Brucker advance DPX 400 MHz with tetramethylsilane as an internal standard was used to record ^{1}H-NMR spectra in $CDCl_3$ (δ in ppm) at WMSRC, JU, Bangladesh. XRD patterns were obtained from CARS, University of Dhaka, Bangladesh. Thin-layer chromatography (TLC) was performed on Kieselgel GF254, and visualization was achieved by spraying plates with 1% H_2SO_4 followed by heating the plates at 150–200 °C until coloration occurred. Column chromatography was performed with silica gel G60. $CHCl_3$/CH_3OH was employed as the solvent system for TLC analyses was in different proportions. All reagents used were commercially available (Aldrich) and used without further purification unless otherwise specified.

Synthesis

In dry DMF (N,N-dimethylformamide) (3 ml), a cytidine (1) (70 mg, 0.287 mmol) solution was cooled to −5° C when decanoyl chloride (65 mg, 1.1 molar eq.) was added. The solution was stirred at this temperature for 5 to 6 h and then was allowed to stand at room temperature overnight. Reaction progress was monitored through TLC, which indicated the complete conversion of the starting material into a single product. A few pieces of ice were added to the flask to stop the reaction. Subsequently, the solvent was evaporated using a high-pressure vacuum evaporator, and the resulted product was passed through silica gel column chromatography and eluted with (1:24), which provided the decanoyl derivative (2) (92 mg). The recrystallization of ($CHCl_3$–C_6H_{14}) led to the formation of the title derivative (2) as needles. The derivative was sufficiently pure for subsequent use without further treatment and identification.

Scheme-1

5′-O-Decanoylcytidine (2)

Yield 83.8% as crystalline solid, M.P. 85–87 °C ($CHCl_3$–C_6H_{14}), Rf = 0.51 (CHCl3/CH3OH = 24/1, v/v). FTIR: νmax 1731, 1714 (-CO), 3550 (-NH), 3420 cm^{-1} (-OH). 1H -NMR (400 MHz, CDCl3): δH 9.02 (1H, s, -NH), 7.44 (1H, d, J = 7.8 Hz, H-6), 6.56 (1H, d, J = 3.0 Hz, H-1′), 6.49 (1H, s, 2′-OH), 6.01 (1H, dd, J = 2.4 and 12.3 Hz, H-5′a), 5.56 (1H, dd, J = 2.4 and 12.3 Hz, H-5′b), 5.45 (1H, s, 3′-OH), 4.85 (1H, dd, J = 2.4 and 5.6 Hz, H-4′), 4.60 (2H, s, $-NH_2$), 4.45 (1H, d, J = 3.2 Hz, H-2′), 4.31 (1H, dd, J = 3.6 and 5.8 Hz, H-3′), 3.80 (1H, d, J = 7.2 Hz, H-5), 2.38 {2H, m, $CH_3(CH_2)7CH_2CO$-}, 1.59 {2H, m, $CH_3(CH_2)6CH_2CH_2CO$-}, 1.32 {12H, m, $CH_3(CH_2)6(CH_2)2CO$-}, 0.85 {3H, m, $CH_3(CH_2)8CO$-}. MS [M+1]+ 398.10. Anal Calcd. for $C_{19}H_{31}N_3O_6$: % C, 72.54, H, 7.81; found: % C, 72.53, H, 7.82.

General procedure for the direct 2',3'-di-O-acylation of 5′-O-decanoylcytidine (2) derivatives (3–7)

In DMF (3 mL), octanoyl chloride (0.185 mL, 4 molar eq.) was added to a cooled (0 °C) and stirred solution of the decanoyl derivative (2) (110 mg, 0.276 mmol). The mixture was stirred at 0 °C for 8 h and then allowed to stand overnight at room temperature. TLC analyses showed the complete conversion of reactants into a single product. A few pieces of ice were added to the reaction flask to eliminate the excess reagent, and the reaction mixture was evaporated using the high-pressure vacuum evaporator to remove the solvent. The percolation of the resulting product achieved by passing through a silica gel column with the $CHC1_3$–CH_3OH eluant led to the formation of the octanoyl derivative (3) (163 mg) as a crystalline solid. A similar reaction and purification procedure were employed to prepare derivatives 4, 5, 6, and 7.

5′-O-Decanoyl-2′,3′-di-O-octanoylcytidine (3)

Yield 77.6% as a white crystalline solid, M.P. 89–91 °C ($CHCl_3$–C_6H_{14}), Rf = 0.51 ($CHCl_3$/CH_3OH = 24/1, v/v). FTIR: νmax 1729, 1716 (-CO), 3470 cm^{-1} (-NH). ^{1}H-NMR (400 MHz, $CDCl_3$): δH 9.18 (1H, s, -NH), 7.27 (1H, d, J = 7.8 Hz, H-6), 6.54 (1H, d, J = 3.2 Hz, H-1′), 5.45 (1H, m, H-2′), 4.82 (1H, dd, J = 3.5 and 5.6 Hz, H-3′), 4.67 (1H, dd, J = 2.4 and 12.2 Hz, H-5′a), 4.58 (2H, s, $-NH_2$), 4.55 (1H, dd, J = 2.4 and 12.2 Hz, H-5′b), 4.38 (1H, dd, J = 2.4 and 5.5 Hz, H-4′), 3.70 (1H, d, J = 7.2 Hz, H-5), 2.37 {4H, m, 2 × $CH_3(CH_2)5CH_2CO$-}, 1.64 {4H, m, 2 × $CH_3(CH_2)4CH_2CH_2CO$-}, 1.29 {16H, m, 2 × $CH_3(CH_2)_4(CH_2)_2CO$-}, 0.89 {6H, m, 2 × $CH_3(CH_2)_6CO$-}. MS [M+1]+ 650.09. Anal Calcd. for $C_{35}H_{59}O_8N_3$: % C, 64.71, H, 9.09; % found: C, 64.73, H, 9.06.

Scheme-2

In dry DMF (3 mL), a cytidine (1) (70 mg, 0.287 mmol) solution was cooled to −5 °C and treated with 1.1 molar equivalent of triphenylmethyl chloride (85 mg) with continuous stirring at the same temperature for 5 to 6 h. Stirring was continued overnight at room temperature. Reaction progress was monitored through TLC. A few pieces of ice were added to the flask to terminate the reaction. Subsequently, the solvent was evaporated using the high-pressure vacuum evaporator. The resulting syrupy mass was purified through silica gel column chromatography (with $CHCl_3$–CH_3OH, 1:24 eluant) to acquire the title derivative (8, 107 mg) as a crystalline solid.

5′-O-(Triphenylmethyl)cytidine (8)

Yield 81.2% as a white crystalline solid, M.P. 75–77 °C) ($CHCl_3$–C_6H_{14}), Rf = 0.50 ($CHCl_3$/CH_3OH = 24/1, v/v). FTIR: νmax 1701 (-CO), 3547 (-NH), 3416-3468 (br) cm^{-1} (-OH). ^{1}H -NMR (400 MHz, $CDCl_3$): δH 9.01 (1H, s, -NH), 7.35 (6H, m, Ar-H), 7.30 (9H, m, Ar-H), 7.23 (1H, d, J = 7.8 Hz, H-6), 6.61 (1H, d, J = 3.0 Hz, H-1′), 6.48 (1H, s, 2′-OH), 5.30 (1H, dd, J = 2.2 and 12.2 Hz, H-5′a), 5.26 (1H, dd, J = 2.2 and 12.2 Hz, H-5′b), 5.15 (1H, s, 3′-OH), 4.85 (1H, dd, J = 2.2 and 5.6 Hz, H-4′), 4.50 (2H, s, -NH_2), 4.25 (1H, d, J = 3.2 Hz, H-2′), 4.01 (^{1}H, dd, J = 3.6 and 5.8 Hz, H-3′), 3.91 (1H, d, J = 7.2 Hz, H-5). MS [M+1]+ 486.08. Anal Calcd. for $C_{28}H_{27}O_5N_3$: % C, 69.28, H, 5.56; % found: C, 69.27, H, 5.53.

General procedure for the direct 2′,3′-di-O-acylation of 5′-O-(triphenylmethyl)cytidine derivatives (9–15) The triphenylmethyl derivative (8, 60 mg, 0.124 mmol) was dissolved in dry DMF (3 mL), and the solution was cooled to 0 °C when hexanoyl chloride (0.067 mL, 4 molar eq.) was added. The mixture was stirred at 0 °C for 6 h and room temperature overnight. The conventional work-up procedure and subsequent chromatographic purification with the $CHCl_3$–CH_3OH (1:24) eluent led to the formation of 2',3'-di-O-hexanoyl derivative (9, 157 mg).

2′,3′-Di-O-hexanoyl-5′-O-(triphenylmethyl)cytidine (9)

Yield 81.5% as crystalline solid, M.P. 100–102 °C, Rf = 0.52 ($CHCl_3$/CH_3OH = 22/1, v/v). FTIR: νmax 1710 (-CO), 3503 cm^{-1} (-NH). ^{1}H-NMR (400 MHz, $CDCl_3$): δH 9.08 (^{1}H, s, -NH), 7.32 (6H, m, Ar-H), 7.28 (9H, m, Ar-H), 7.21 (1H, d, J = 7.6 Hz, H-6), 6.51 (1H, d, J = 3.2 Hz, H-1′), 5.47 (^{1}H, m, H-2′), 4.88 (1H, dd, J = 3.2 and 5.4 Hz, H-3′), 4.61 (^{1}H, dd, J = 2.2 and 12.2 Hz, H-5′a), 4.54 (2H, s, -NH_2), 4.48 (^{1}H, dd, J = 2.2 and 12.2 Hz, H-5′b), 4.35 (^{1}H, dd, J = 2.2 and 5.4 Hz, H-4′), 3.81 (^{1}H, d, J = 7.1 Hz, H-5), 2.31 {4H, m, 2 × $CH_3(CH_2)_3CH_2CO$-}, 1.62 {4H, m, 2 × $CH_3(CH_2)_2CH_2CH_2CO$-}, 1.26 {8H, m, 2 × $CH3(CH_2)_2CH_2CH_2CO$-}, 0.88 {6H, m, 2×$CH_3(CH_2)_4CO$-}. MS [M+1]+ 682.05. Anal Calcd. for $C_{40}H_{47}O_7N_3$: % C, 70.40, H, 6.90; % found: C, 70.42, H, 6.91.

A similar reaction and purification method were employed to synthesize derivatives 10 (164 mg), 11 (152 mg), 12 (109.5 mg), 13 (100.4 mg), 14 (132 mg), and 15 (111 mg).

Pathogenicity test

Antibacterial and antifungal activity

The newly acylated cytidine derivatives (schemes 1 and 2) were screened for in vitro antibacterial activity

against five human pathogenic bacteria by using the disk diffusion method (Bauer *et al.* 1966). In this method, paper disks and a glass Petri plate of 4 and 90 mm, respectively, in diameter were used throughout the experiment. Sterile dimethyl sulfoxide (DMSO) was employed to prepare the desired concentrations of the synthesized compounds and standard antibiotics. The paper disks were soaked with test chemicals at a rate of 0.2 mg (dry weight) per disk for the antibacterial analysis. The bacterial suspensions were swabbed with Mueller–Hinton Agar (MHA) media and then sterile soaked disks were placed on it. First, the plates were maintained at low temperature (4 °C) for 4 h, and the test chemicals diffused from the disks into the surrounding media by this time. The plates were then incubated at 37 °C for test organism growth and were observed at intervals of 24 h for two days. Azithromycin acquired from Asiatic Laboratories Ltd. (Bangladesh) was used as the positive control, and DMSO was used as the negative control.

The MIC and MBC were determined using the two-fold broth dilution technique (Amsterdam 2005). In this method, a change in the color from yellow to pink-red indicated bacteria growth, and MIC was interpreted visually. The next highest MIC dilution, at which at least 99% of bacteria were inhibited to grow, was considered the MBC that was confirmed by bacterial growth on MHA. In a certain row, the first well was treated as the negative control without using any chemicals, and the eighth well was treated as the positive control by using standard antibiotic azithromycin.

The in vitro antifungal mycelial growth activity of the test derivatives was determined using the "poisons food" technique (Grover and Moore 1962). A required amount of medium was separately taken in a conical flask and sterilized in an autoclave. After the autoclaving process, the weighed amount of test chemicals (in DMSO to a 1% to 2% (w/v)) was added to the sterilized medium in the conical flask at the point of pouring to obtain the desired concentration. The flask was shaken thoroughly to homogeneously mix the chemical with the medium before pouring. The medium with a definite concentration (2%) of the chemical was individually poured at the rate of 10 µl in the sterilized glass Petri dishes. Proper control was maintained separately with the sterilized PDA medium without compounds, and three replications were prepared for each treatment. The percentage inhibition of the mycelia growth of the test fungus was calculated as follows:

$$I = \frac{C\text{-}T}{C} \times 100 \quad (1)$$

where I is the percentage of inhibition, C represents the diameter of the fungal colony in the control (DMSO), and T is the diameter of the fungal colony during the treatment.

Anticancer activity by EAC cells

According to the method of Hasan et al. (Hasan et al. 2019), the MTT colorimetric assay with slight modifications was used to detect the proliferation of Ehrlich's ascites carcinoma (EAC) cells. In a 96-well flat-bottom culture plate, 5 × 105 EAC cells (5 × 105 in 200 µl of RPMI-1640 media) were plated in the presence and absence of different concentrations of derivative 6 (12.5–200 µg/mL) and incubated at 37 °C in a CO_2 incubator for 24 h. After the removal of the aliquot from each well, 180 µl of PBS (Phosphate-buffered saline) and 20 µl of MTT (5 mg/mL) were added to the 96-well plate and incubated at 37 °C for 4 h. Subsequently, the aliquot was removed again and 200 µl of acidic

isopropanol was added to each well. The plate was agitated for 5 min, and then the absorbance was measured at 570 nm by using a titer plate reader. The following equation was used to calculate the cell proliferation inhibition ratio:

$$\text{Proliferation inhibition ratio (\%)} = \{(A - B) \times 100\}/A \quad (1)$$

where, A and B are the OD570 nm of the cellular homogenate (control) without and with derivative 6, respectively.

X-ray powder diffraction

X-ray powder diffraction was performed using Rigaku Dmax2200PC diffractometer (Rigaku Corporation, Tokyo, Japan) and Cu Kα-radiation. The X-ray intensity was measured in the range of $5° \leq 2\theta \leq 90°$ with a scan speed of $2°\cdot min^{-1}$. The peak position of the 002 coke peak was measured. By using Bragg's law, the interlayer d-spacing was calculated. The improved Langford method was employed to calculate the stacking disorder degree, P.

Structure-activity relationship

SAR studies can be conducted to predict the biological activity from the molecular structure of pharmaceutical targets. This powerful technology is frequently used in drug discovery processes to guide the acquisition or synthesis of desirable new compounds and to characterize existing molecules. SAR assays were performed according to the membrane permeation concept of Kim (Kim *et al.,* 2007) and Hunt (Hunt, 1975).

Computational study

Optimization of cytidine derivatives and preparation of protein

In molecular drug design study, quantum mechanical (QM) methods have gained attention on the calculation of thermodynamic properties, molecular orbital features, dipole moment, and as well as interpretation of different types of interactions. Molecular geometry optimization and further modification of all cytidine derivatives carried out using Gaussian 09 program (Chatfield et al. 2002). Density functional theory (DFT) with Beck's (B) three-parameter hybrid model, Lee, Yang and Parr's (LYP) (Lee et al. 1988) correlation functional under 3-21g basis set has been employed to optimize and predict their binding properties. The 3D crystal structure of HIV-1 reverse transcriptase (PDB: 3V4I) was retrieved in pdb format from the protein data bank (Berman et al. 2000). Then optimized cytidine derivatives were subjected for molecular docking study against HIV-1 reverse transcriptase (3V4I) (Fig. 2). In fine, molecular docking simulation was rendered by PyRx software (version 0.8) considering the protein as a macromolecule and the drug as a ligand. After the completion docking, both the macromolecule and ligand structures were saved in. pdbqt format needed by Accelrys Discovery Studio (version 4.1) to explore and visualize the docking result and search the nonbonding interactions between ligands and amino acid residues of the receptor protein.

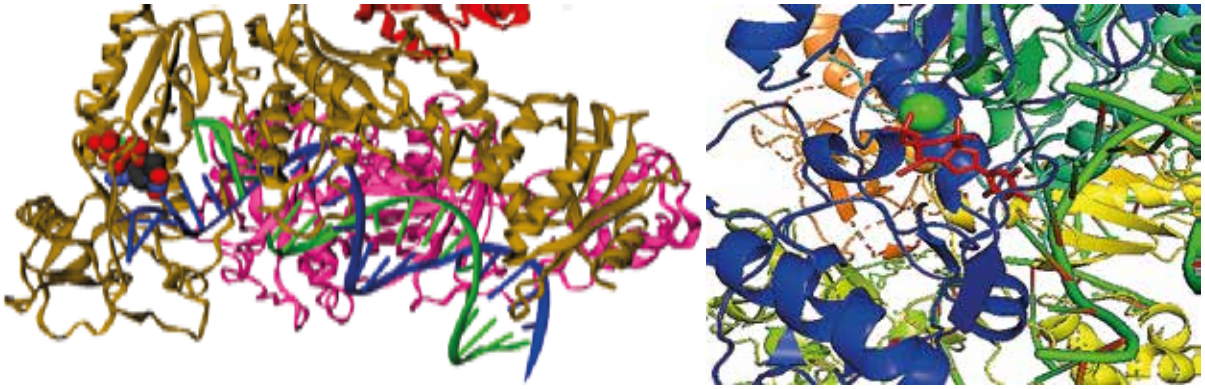

a b

Fig. 2. Crystal structure of HIV-1 reverse transcriptase (RT) (PDB: 3V4I) (a); and the active site of RT (binding site of nucleoside reverse transcriptase inhibitors (NRTI) (b).

Pharmacokinetics prediction

To point out potential drug candidates, the ADMET properties were developed for the preliminary prediction of the pharmacokinetics and toxicity, and drug-like properties in the discovery drug process. In silico study gives a way to the accession of pharmacokinetic parameters (Adsorption, Distribution, Metabolism, Excretion, and Toxicity; ADMET), its absorption in the human intestine, percolation of the blood-brain barrier and the central nervous system, the metabolism indicates the chemical biotransformation of a drug by the body, total clearance of drugs and the toxicity levels of the molecules.

Results and discussion

Chemistry

In this study, regioselective decanoylation (scheme 1) and triphenylmethylation (Scheme 2) of cytidine (1) were performed using the direct method. The resulting decanoylation and triphenylmethylation products were converted into numerous derivatives by employing various acylating agents.

Characterization and selective decanoyl of cytidine (scheme-1)

Cytidine 1 was initially converted into the 5′-O-decanoylcytidine derivative 2 through treatment with dry pyridine, and this product after the reaction with decanoyl chloride, followed by solvent removal and silica gel column chromatographic purification, produced 5/-O-decanoyl derivative (2) with good yield. The FTIR spectrum of derivative 2 showed the following absorption bands: 1731, 1714 cm−1 (due to –CO), 3420 cm^{-1} (due to –OH), and 3550 cm^{-1} (due to –NH) stretchings. The two multiplets were observed at δ 2.3 and 1.59 which corresponded to $–CH_2$ groups adjacent to –CO groups, and$–CH_2$ groups adjacent to $–CH_2CO$ groups of decanoyl groups, respectively. A 12H multiplet appeared at δ 1.32 assigned to 6 equivalents $–CH_2$ groups of decanoyl groups. A 3H multiplet dictated at δ 0.85 ascribed to $–CH_3$ groups

of dodecyl groups attached at C-5′ position of compound (2). The downfield shift of C-5/ proton to δ 6.01 (as dd, J = 2.4 and 12.3 Hz, H-5′a) and to δ 5.56 (as dd, J = 2.4 and 12.3 Hz, H-5′b) from their general values in the precursor derivative 1 and the resonances of other protons in their anticipated positions indicated the presence of the decanoyl group at position 5/. The formation of 5′-O-decanoylcytidine 2 might be caused by the high reactivity of the sterically less hindered primary hydroxyl group of the ribose moiety of cytidine 1. Mass spectrometry provided a molecular ion peak at m/z [M+1]+ 398.10, which corresponded to the aforementioned molecular formula. From the complete analysis of FTIR, ^{1}H-NMR, and elemental data, the structure of this derivative was assigned as 5′-O-decanoylcytidine 2.

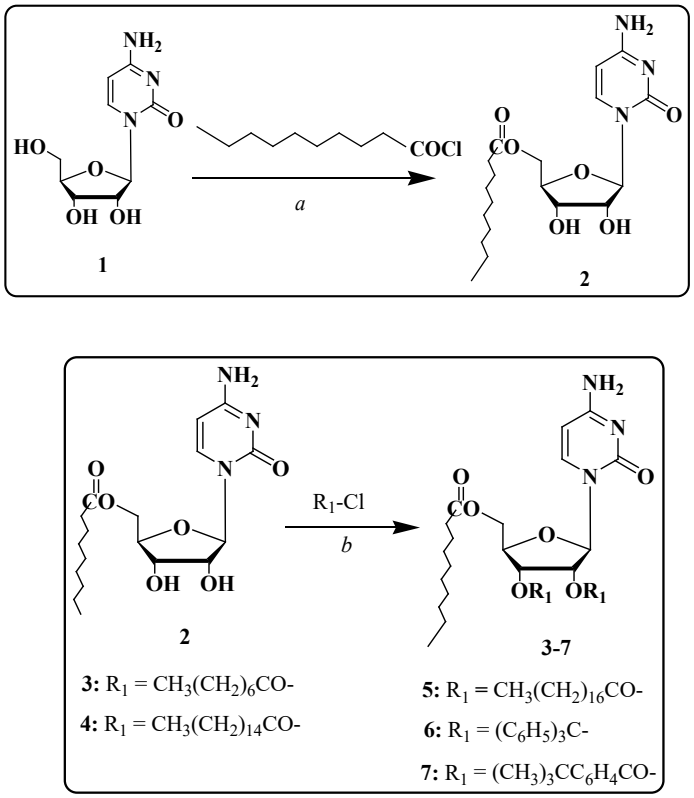

Scheme 1. Reagents and conditions: (a) dry C_6H_5N, −5 °C, 6 to 7 h, decanoyl-, (b) DMAP, stir for 6–8 h, R1 = different acyl halides (3–7).

Scheme 1. Reagents and conditions: (a) dry C_6H_5N, −5 °C, 6 to 7 h, decanoyl-, (b) DMAP, stir for 6–8 h, R1 = different acyl halides (3–7).

Furthermore, the structure of derivative 2 was confirmed through the preparation of its octanoyl derivative 3. In its ^{1}H-NMR spectrum, the two multiplets were accomplished at δ 2.37 and 1.64 which corresponded to –CH_2 groups adjacent to –CO groups and –CH_2 groups adjacent to –CH_2CO groups of octanoyl groups, respectively. A 16H multiplet appeared at δ 1.29 assigned to 8 equivalents –CH_2 groups of octanoyl groups. A 6H multiplet dictated at δ 0.89 ascribed to –CH3 groups of octanoyl groups attached at C-5′

position of compound (3). The structure of octanoyl derivative (3) was confirmed as 5′-O-decanoyl-2′,3′-di-O-octanoylcytidine (3) through the complete analysis of their FTIR, ^{1}H-NMR, and elemental data. The decanoyl derivative 2 was further transformed easily into the 2′,3′-di-O-palmitoyate 4, 2′,3′-di-O-stearoyate 5, 2′,3′-di-O-(triphenylmethyloate) 6, and 2′,3′-(4-tert-butylbenzoate) 7 with excellent yields.

Characterization and selective triphenylmethylation of cytidine (scheme-2)

Cytidine (1) was then transformed into the 5′-O-(triphenylmethyl)cytidine derivative 8 through a treatment with a unimolecular amount of triphenylmethyl chloride in anhydrous pyridine at −5 °C. The conventional work-up procedure, followed by solvent removal and silica gel column chromatographic purification, produced high yields of the triphenylmethyl derivative 8 as the crystalline solid. In its 1H-NMR spectrum, two characteristic six-proton multiplets appearing at δ 7.35 (Ar–H) and nine-proton multiplets observed at δ 7.30 (Ar–H) were caused by three phenyl protons of the triphenylmethyl group in

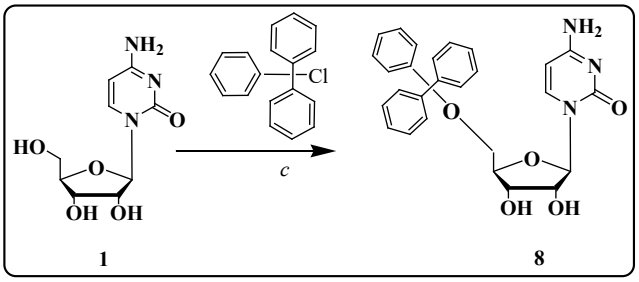

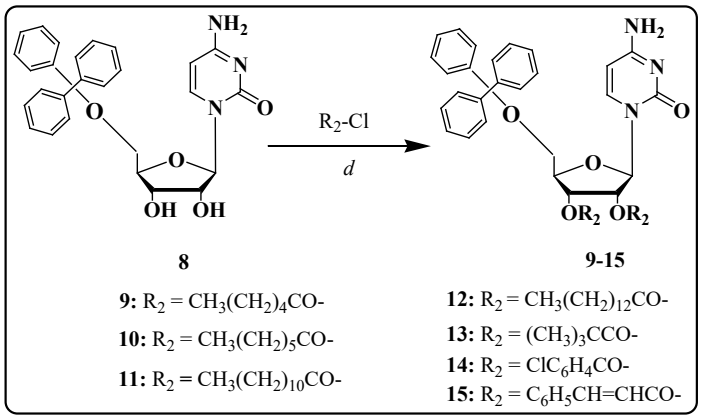

Scheme 2. Reagents and conditions: (c) dry C_6H_5N, 0–5 °C, 6 h, triphenylmethyl-, (d) DMAP, stir for 6 to 7 h, R2 = several acyl halides (9–15).

the molecule. This finding is in accordance with the mechanism proposed by Bulbul *et al.* (2021) based on similar nucleoside derivatives.

The preparation and identification of hexanoyl derivative 9 further supported the structure of derivative 8. A derivative 8 was then converted into heptanoyl derivative 10 by using similar procedures, and a high yield of heptanoate 10 was isolated as needles. From the complete analysis of the FTIR, ^{1}H-NMR, and elemental data, the structure of this compound was confirmed as 2′,3′-di-O-heptanoyl-5′-O-(triphenylmethyl)cytidine (10). Similarly, derivative 8 was converted into numerous acylated derivatives (11–15) to obtain newer compounds for antimicrobial and anticancer screening studies. The structures of these derivatives were ascertained through the complete interpretation of their FTIR and ^{1}H-NMR spectra.

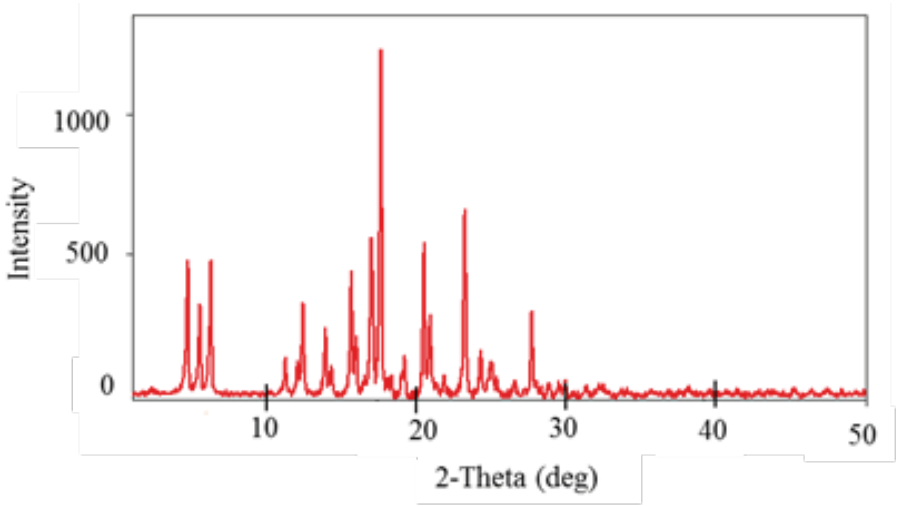

Fig. 3. XRD pattern of 2′,3′-di-*O*-pivaloyl-5′-*O*-(triphenylmethyl)cytidine (13).

XRD measurements

The XRD patterns of the pure compounds synthesized under the optimized conditions were obtained in the 2θ range of (0°–50°). According to the phase analysis, the compounds synthesized using this method have high purity, and no impurities were detected in the XRD pattern. Moreover, derivatives 4, 5, 13, and 15 show many lines with high intensity in their XRD patterns, which indicated that all the derivatives are highly crystalline (Fig. 3).

Pathogenicity activities

This antibacterial activity screening test suggests that the incorporation of various new acyl groups in cytidine (1) increased the antibacterial activity of these compounds noticeably. The test derivatives exhibited promising inhibitory activity against both the Gram-positive and Gram-negative bacterial strains. The inhibition data indicated that derivatives 7, 10, and 11 were more active against *B. subtilis* and *S. aureus* than the standard antibiotic, Ampicillin was. Furthermore, derivative 7 showed the

highest activity against *B. subtilis*, which was higher than that of the standard drug, among all tested organisms. However, acylated derivatives 2, 4, 5, and 13 showed either slight inhibition or did not show any inhibition against the bacterial strains examined. Derivatives 3, 7, 10, and 15 were highly active against both the Gram-positive and Gram-negative organisms. The starting cytidine 1 did not show any activity against any tested bacteria. This variation in the antibacterial activity of the examined compounds may be caused by the incorporation of diverse acyl groups into cytidine molecules. From the recorded MIC and MBC values, it can be concluded that the derivatives 7, 10, and 11 (i.e. 4-t-butylbenzoyl, heptanoyl, and lauryl derivatives) were found highly active against *Bacillus subtilis* bacterium as all the derivatives showed minimum MIC value (0.3125 mg/mL) against *Bacillus subtilis.* These three derivatives also have the same MBC value (1.25 mg/mL) against most of the bacteria (Misbah *et al.* 2020). The antifungal screening data suggested that derivatives 6 (68.06 ± 0.9%), 10 (76.13 ± 1.8%), and 14 (80.66 ± 1.1%) showed marked toxicities toward *A. niger*, which were even higher than the toxicity of the standard antibiotic, nystatin (66.40 ± 1.8%). By contrast, derivative 13 (60 ± 1.9%) showed excellent inhibition against *A. flavus*, which was comparable to inhibition by nystatin (63.10 ± 1.9%). The designed derivatives 12–14 (myristoyl, pivaloyl, and 4-chlorobenzoyl) showed activity against both A. niger and A. flavus. The rest of the derivatives 1–3, 7–9, 11, and 15 showed no activity against both tested fungi. The remaining tested derivatives were also showed a moderate to considerable antifungal activity. The incorporation of myristoyl, pivaloyl, and 4-chlorobenzoyl groups at C-5′ and C-2,3′-di-O-positions of the tested compounds increased their antifungal activity against tested organisms, which is considerab similar by our previous findings (Kawsar *et al.* 2014).

Anticancer activities

MTT assay was used to investigate the effect of derivatives 3-15 in vitro on EAC cells. Among the all tested derivatives, the derivative 6 [5′-O-decanoyl-2′,3′-di-O-(triphenylmethyl)cytidine] was obtained potentially active. The EAC cell death was found to be dose-dependent manner. When the concentration decreased gradually, the inhibitory effect also reduced and finally reached to 1.32% at 15.625 µg/mL of the derivative 6. Therefore, derivative 6 can be used as an anticancer drug mentioning further investigation. The results showed that some of the newly synthesized acylated cytidine derivatives possess a wide range of antimicrobial activities and that the antimicrobial activities of cytidine derivatives depend on the type of substituents, the length of alkyl chains, and the number of acyl rings. Thus, cytidine derivatives (2–15) may be considered potential sources for developing new and better antimicrobial agents against numerous human and plant pathogenic microorganisms.

SAR study

We attempted to determine the SAR of the tested compounds on the basis of in vitro experimental results. The incorporation of different acyl groups, especially in the C-5′ position and later in C-3′ and C-2′ positions, increases the activity of the tested chemicals against bacteria and fungus. The test chemicals with more hydrophobic groups in their structure show higher activity than precursor 1, which shows relatively lower activity due to the presence of three free hydroxyl groups. Furthermore,

when the hydroxyl group of C-5′ is blocked by a triphenylmethyl group and two hydroxyl groups, especially when C-2′ and C-3′ remain free, then derivative 8 shows little activity (16 mm zone of inhibition against *B. subtilis*). The presence of different acyl groups instead of hydroxyl groups also leads to antibacterial activity enhancement.

Compound 11 contains a triphenylmethyl group at the C-5′ position and a lauroyl group at C-2′ and C-3′ positions and shows the highest zone of inhibition of 27 mm against B. subtilis. However, derivative 8 contains a decanoyl group at the C-5′ position and an octanoyl group at C-2′ and C-3′ positions and shows a high zone of inhibition of 21 mm against *B. subtilis*. The hydrophobicity of materials as toxicity or alteration of membrane integrity is an important parameter with respect to bioactivity because it is directly related to membrane permeation (Kim *et al.* 2007). Hunt (Hunt 1975) reported that the potency of aliphatic alcohols is directly related to their lipid solubility through hydrophobic interactions between the alkyl chains of alcohols and lipid regions in the membrane.

As a consequence of their hydrophobic interactions, bacteria lose their membrane permeability, ultimately leading to bacterium death. Therefore, the activity order is 11 > 8 > 3 against *B. subtilis*. This result concluded that not only hydrophobicity but also aromatic nuclei increase the antibacterial activity of chemical substances. This finding led us to conclude that the incorporation of 2′,3′-di-O-octanoyl/lauroyl groups in the cytidine framework along with 5′-O-decanoyl/or triphenylmethyl groups increased the antimicrobial potentiality of cytidine 1.

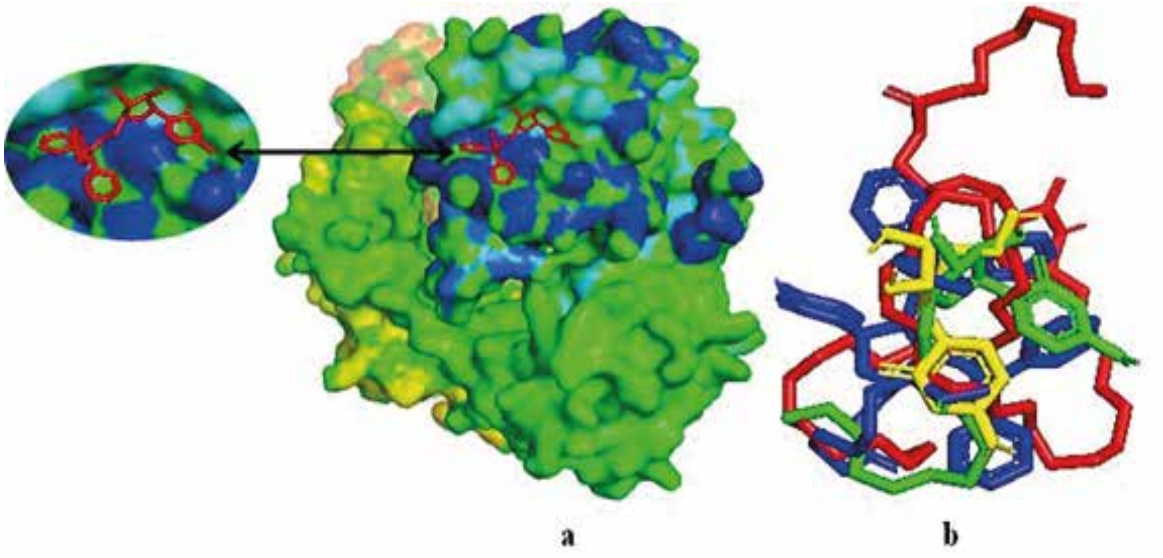

Fig. 4. Docked conformation of derivative (10) at the inhibition binding site of HIV-1 reverse transcriptase (RT) (3V4I) (a); superimposed view of all the derivatives after rigid docking (b).

Molecular docking studies

Calculation of the feasible binding geometries and interactions between drugs and active site of proteins obtained from molecular docking. By using the Autodock Vina 4.2.6, molecular docking was performed to suggest the best candidates among the selected cytidine derivatives 2-15 based on their binding affinities. All selected molecules were subjected to docking into the same binding pocket of HIV-1 reverse transcriptase (RT) (PDB: 3V4I) using similar optimized docking conditions to identify their binding mode. The results of the docking exploration showed that all cytidine derivatives, along with the parent molecule, gain binding affinities ranging from -4.5 to -8.3 kcal/mol. It was found that the derivatives 2-7 and 9-12 showed low binding affinities compared to the parent, cytidine, while derivatives 8, 13, 14, and 15 exhibited high binding affinity. These results revealed that modification of –OH group at position 2′,3

Table 1. In silico ADMET prediction of cytidine and its derivatives

Entry	Absorption	Distribution			Metabolism						Excretion
	Intestinal absorption (human)	VDss (human)	BBB permeability	CNS permeability	Substrate		Inhibitor				Total Clearance
					CYP						
					2D6	3A4	1A2	2C19	2D6	3A4	
	Numeric (% Absorbed)	Numeric (Log L/kg)	Numeric (Log BB)	Numeric (Log PS)	Categorical (Yes/No)						Numeric (Log ml/min/kg)
2	55.307	-0.432	-1.137	-4.347	No	Yes	No	Yes	No	Yes	1.458
3	73.955	0.064	-0.983	-3.339	No	Yes	Yes	Yes	No	Yes	1.367
4	100.00	0.491	0.348	-2.186	No	Yes	Yes	Yes	No	Yes	1.614
5	100.00	0.506	0.234	-2.139	No	Yes	Yes	Yes	No	Yes	1.677
6	100.00	0.428	0.307	-2.715	No	Yes	Yes	Yes	No	Yes	0.109
7	83.476	0.042	0.361	-3.574	No	Yes	No	Yes	No	Yes	0.028
8	70.682	-1.463	-0.853	-3.621	No	Yes	Yes	Yes	No	Yes	0.276
9	100.00	0.498	0.272	-1.575	No	Yes	Yes	Yes	No	Yes	0.639
10	100.00	0.494	0.114	-1.512	No	Yes	Yes	Yes	No	Yes	0.660
11	100.00	0.427	0.131	-1.252	No	Yes	Yes	Yes	No	Yes	0.810
12	100.00	0.379	0.017	-1.205	No	Yes	Yes	Yes	No	Yes	0.846
13	100.00	0.402	0.243	-2.403	No	Yes	Yes	Yes	No	Yes	0.641
14	93.416	0.225	0.190	-2.337	No	Yes	Yes	Yes	No	Yes	-0.386
15	91.246	0.204	0.233	-2.878	No	Yes	Yes	Yes	No	Yes	0.696

′,5′of cytidine structure, along with an aromatic ring or an aliphatic chain molecule improved the binding affinity, while the insertion of halo-benzoyl groups like Cl- and Br-, made some fickleness in binding affinities. However, modification with either an aromatic ring or halogenated aromatic rings increased the binding affinity. The docked pose showed that the drug molecules bind within the active site of the HIV-1

reverse transcriptase (RT) (3V4I) macromolecular structure (Fig. 4).

Molecular docking showed that cytidine derivatives 7, 8, 14, and 15 (binding affinities -6.3, -8.1 -8.3 and -7.2 kcal/mol) binds firmly through hydrophobic bonds with the catalytic binding site Tyr181, Val35, Val90, Val179, Val381, Lys32, and Ile31, where, these residues exhibited alkyl, pi-alkyl pi-sigma pi-pi T-shaped and amide-pi stacked interaction. This pi-pi interaction revealed the tight binding with the active site. Again, Gln91, Gln161, Tyr144, Ile142 (shorter distance 1.88046 Å), Val90, and Thr165 which are the highly specific binding pocket of HIV-1 reverse transcriptase (RT) found to form a hydrogen bond. An electrostatic bond (Pi-cation) was also found with Lys172 and Lys374 at compounds 7 and 15. It is evident from the structural contrast compound 7-8 and 14-15 have an additional aromatic (4-tert-butylbenzoyl, tri-phenyl ring, halogenated ring, and cinnamoyl ring) substituent in the parent structure, indicating a high density of electron in the molecule leading to a comparatively higher binding affinity -6.3 to - 8.3 kcal/mol. Binding affinity and binding specialty are improved in the case of (2, 5, 6, 7, 8, 10, 13, and 14) due to significant hydrogen bonding. It was observed that modifications of the –OH group of cytidine (1) enhanced the π-π interactions with the residues of the active site while increasing their polarity resulted in the formation of hydrogen bonding interactions. The most prominent H-bonds were obtained for the derivatives (5 and 12), forming with Ala355, Gln332, Thr338, Arg356, and Asn265. Hydrogen bonds execute a vital function in shaping the specificity of ligand binding with the receptor, drug design in chemical and biological processes, molecular recognition, and biological activity (Perlstein et al. 2001). Among all the molecules, the inhibition activity of the esters (8, 14, and 15) was found to be the highest (-8.1,-8.3, and -7.2 kcal/mol). The results were summarized into a set of structural changes to be used in HIV-1 reverse transcriptase inhibitor design: cytidine esters gave an improved affinity and inhibitory potential, because of their relative flexibility combined with a favorable interaction with the active site.

Pharmacokinetic analysis

All newly modified cytidine derivatives have potential activities. Therefore, to ensure that the modified esters are the viable drugs, we used the in silico pharmacokinetic parameters ADMET. The pkCSM online server (Pires et al. 2015) was employed to calculate in silico ADMET properties (Table 1). Absorbance value below 30% indicates poor absorbance, here esters 4-6 and 9-13 are displaying a value of 100% and 14-15 displaying >90% which reveals a good absorbance in the human intestine.

The volume of distribution (VDss) is thought high if the value is higher than 0.45. In addition, blood-brain barrier (BBB) and central nervous system (CNS) permeability standard values (>0.3 to < -1 Log BB and > -2 to < -3 Log PS), respectively. For a given compound a Log BB < -1 is poorly distributed to the brain, while Log BB >0.3 are the potential to cross BBB and LogPS > -2 considered to penetrate the CNS, while Log PS < -3 are difficult to move in the CNS. It was observed that most of the compounds have the best significant potential to cross the barriers except esters 2, 3, and 8. The enzymatic metabolism ensures the chemical biotransformation of a designed drug in the body, which plays a key role in the transformation of drug compounds. In the body,

drugs produce several enzymatic metabolites, which plays role in catalyzing the reaction with several drug concentrations. It is essential to consider their metabolism of drugs, which may show several physicochemical and pharmacological parameters. The cytochrome P450 (CYP450) plays a major role in drug metabolism because the major liver enzyme system is involved in phase 1 metabolism. Some selective CYP genes CYP1, CYP2, CYP3, and CYP4 families are found to be involved in drug metabolism, with CYP (1A2, 2C19, 2D6, and 3A4) being causes the biotransformation of greater than 90% of drugs undergoing phase I metabolism.

Conclusion

In this study, we report an efficient acylation of novel cytidine derivatives by the direct method. This direct method demonstrates a very simple and efficient method for the synthesis with excellent yields and short reaction times. The synthesized cytidine derivatives have shown promising antibacterial and antifungal activities which were further rationalized by the SAR study. Derivatives 7, 10, and 14 were displayed good antimicrobial inhibition activity. However, compound 6 has shown significant anticancer activity against EAC cells by MTT assay. Molecular docking is successfully employed to suggest the best HIV-1 resistance against HIV-1 reverse transcriptase (RT). All of the studied cytidine molecules showed an interesting range of binding affinity -4.5 to-8.3 kcal/mol and strong interactions with at least one of the catalytic residues of the HIV-1 reverse transcriptase (RT), whose are responsible for which causes acquired immunodeficiency syndrome. These blind molecular docking analyses may provide a potential approach for the application of antivirals drugs as expected inhibitors HIV-1 reverse transcriptase. In fine, these derivatives were analyzed for their pharmacokinetic properties which expressed the promising in silico ADMET predictions. In this promising investigation, more drug-likeness in vitro and in vivo studies such as nontoxic concentration towards healthy cells may be conducted in the future.

Acknowledgment

The authors are grateful to the Ministry of Science and Technology, the Government of the People's Republic of Bangladesh for providing financial support (Ref.: 39.00.0000. 09.06.024.19/Phy's-544-560, 2019-2020) to conduct this research.

References

Amsterdam D 2005. In Lorian V, Ed., Antibiotics in laboratory medicine, 6th Ed. Williams L, Wilkins, Philadelphia, p 61.

Arifuzzaman M, Islam MM, Rahman MM, Mohammad AR, Kawsar SMA 2018. *ACTA Pharm. Sci.* **56:** 7–22.

Bauer AW, Kirby WMM, Sherris JC and Turck M 1966. *Am. J. Clin. Pathol.* **45:** 493-496.

Berman HM, Westbrook J, Feng Z, Gilliland G, Bhat TN and Weissig H 2000. *Nucleic Acids Res.* **28:** 235-242.

Bulbul MZH, Chowdhury TS, Misbah MMH, Ferdous J, Day S, Hasan I, Fujii Y, Ozeki Y, Kawsar SMA 2021.

Pharmacia. 68: 23–34.

Chatfield D and Christopher JC 2002. *Theor. Chem. Acc.* **108:** 367-368.

Chowdhury TS, Ferdous J, Misbah MMH, Bulbul MZH and Kawsar SMA 2019. *J. Bang. Chem. Soc.* **31:** 40-48.

Devi SR, Jesmin S, Rahman M, Manchur MA, Fujii Y, Kanaly RA, Ozeki Y and Kawsar SMA 2019. *ACTA Pharm. Sci.* **57:** 47-68.

Groeningen CJ, Leyva A, Kraal I, Peters GJ and Pinedo HM 1986. *Cancer Treat. Rev.* **70:** 745-750.

Grover RK and Moore JD 1962. Phytopathology **52:** 876–879.

Harris KS, Brabant W, Styrchak S, Gall A and Daifuku R 2005. *Antiviral Res.* **67:** 1–9.

Hasan I, Asaduzzaman AKM, Swarna RR, Fujii Y, Ozeki Y, Uddin MB and Kabir SR 2019. *Marine Drugs.* **17:** 502-516.

Hunt WA 1975. Adv. Exp. Med. Biol. **56:** 195-210.

Ichikawa E and Kato K 2001. *Current Med. Chem.* **8:** 385–423.

Ishji H, Nakamura M, Seo S, Tori K, Tozyo T and Yoshimura Y 1980. Chem. Pharm. Bull. **28:** 2367–2373.

Jesmin S, Devi SR, Rahman M, Islam M, Kanaly RA, Fuji Y, Hayashi N, Ozeki Y and Kawsar SMA 2017. *J. Bang. Chem. Soc.* **29:** 12–20.

Jordheim LP, Durantel D, Zoulim F, Dumontet C 2013. *Nat. Rev. Drug Discov.* **12:** 447-464.

Kabir AKMS, Dutta P and Anwar MN 2005. *Chittagong Univ. J. Sci.* **29:** 1–8.

Kabir AKMS, Kawsar SMA, Bhuiyan MMR, Islam MR and Rahman MS 2004. *Bull. Pure Appl. Sci.* **23:** 83–91.

Katherine L, Seley R and Mary KY 2018. *Antiv. Res.* **154:** 66–86.

Kawsar SMA, Faruk MO, Rahman MS, Fujii Y and Ozeki Y 2014. *Sci. Pharm.* **82:** 1-20.

Kawsar SMA, Hosen MA 2020. Turkish Comp, *Theo. Chem.* **4:** 59–66.

Kawsar SMA, Islam M, Jesmin S, Manchur MA, Hasan I and Rajia S 2018. *Int. J. Biosci.* **12:** 211–219.

Kim YM, Farrah S, Baney RH 2007. *Int. J. Antimicrob. Agents.* **29:** 217–222.

King MW 2006. Medical Biochemistry-IU School of Medicine. http://www.miking.iupui.edu

Krayevsky AA and Watanabe KA 1993. Bioinform, Moscow, p 211.

Kukhanova MK 2012. Mol. Biol. **46:** 768–779.

Lee C, Yang W and Parr RG 1988. Phys. Rev. B. **37:** 785-789.

Misbah MMH, Ferdous J, Bulbul MZH, Chowdhury TS, Dey S, Hasan I and Kawsar SMA 2020. *Int. J. Biosci.* **16:** 299-309.

Morris DJ 1994. Drug Safety **10:** 281-291.

Perlstein J 2001. *J. Am. Chem. Soc.* **123:** 191-192.

Pires DEV, Blundell TL, Ascher DB 2015. *J. Med. Chem.* **58:** 4066-4072.

Tanima B, Ritapa C, Krishna SD, Raju M, Subhranshu M and Jyotirmayee D 2019. *ACS Appl. Bio Mater.* **2:** 3171–3177.

Tsuda Y and Haque ME 1983. Chem. Pharm. Bull. **31:** 1437-1439.